Available online at www.sciencedirect.com

SciVerse ScienceDirect

Journal of the European Ceramic Society 33 (2013) 3429–3435

www.elsevier.com/locate/jeurceramsoc

Thermal conductivity of high porosity alumina refractory bricks made by a slurry gelation and foaming method

Toru Shimizu [a,*], Kazuhiro Matsuura [b], Harumi Furue [a], Kunio Matsuzak [a]

[a] *AIST (National Institute of Advanced Industrial Science and Technology), Namiki 1-2-1, Tsukuba, Ibaraki 305-8564, Japan*
[b] *Marukoshi Engineering Corporation, Nu-67 Ishizaki, Nanao, Ishikawa, Japan*

Received 11 October 2012; received in revised form 6 June 2013; accepted 1 July 2013
Available online 27 July 2013

Abstract

Alumina has high heat resistance and corrosion resistance compared to other ceramics such as silica or mullite. However, for its application to refractory bricks, its high thermal conductivity must be reduced. To reduce this thermal conductivity by increasing the porosity, a GS (gelation of slurry) method that can produce high porosity solid foam was applied here to produce the alumina refractory brick. This method was successfully applied to produce alumina foam with high porosity and thermal conductivity of the foam is evaluated. At room temperature, the thermal conductivity was about 0.12 W/mK when the foam density was 0.1 g/cm^3. At elevated temperature above 783 K, thermal conductivity of the foam was strongly affected by heat radiation and increased with increasing temperature, in contrast to the thermal conductivity of alumina itself, which decreased with increasing temperature. The alumina foams developed here achieved sufficient thermal insulating properties for use in refractory bricks.

Keywords: Alumina foam; High porosity; Refractory brick; Hydro-gel; Thermal conductivity

1. Introduction

Recent urgent demands for reduced energy consumption and efficient energy usage require high performance thermal insulation materials.[1] Such demands have been made in the field of refractory materials. Because conventional refractory bricks have good heat resistance performance and can are now being replaced by high performance insulators such as mullite wool or alumina wool. When high heat resistance is not required, either "micro-therm", which has very low thermal conductivity, or low-cost calcium silicate board can be used as such a replacement. However, if the porosity of conventional low-cost refractory bricks can be increased, both the insulation properties and performance at both room temperature and elevated temperature might be improved, and thus refractory bricks can become a viable replacement.

In our present study, a refractory brick whose main components are alumina and ceramic fiber was developed, because alumina has high thermal conductivity, although it requires high porosity to increase its thermal insulation performance. Tradi

foam particles, sawdust and starch[3] are used as fugitive materials. However, the maximum porosity that can be achieved using fugitive or space holder material is only about 60–70%, and the resulting increase in insulation performance is therefore limited. Here, using the GS (gelation of slurry) method that was previously developed to produce high porosity metal foam,[4–6] we produced alumina refractory bricks. We then measured the porosity, mechanical properties (i.e., cell structure and compressive strength), and thermal conductivity of the foam. We also estimated thermal conductivity using modified kunii model. Our results show that this method can successfully produce ceramic foams with porosity from 94 to 98%, and can thus produce high porosity ceramic foams that have low thermal conductivity.

* Corresponding author. Tel.: +81 29 861 7183; fax: +81 29 861 7167.
E-mail address: toru-shimizu@aist.go.jp (T. Shimizu).

0955-2219
http://dx.doi.org/10.1016/j.jeurceramsoc.2013.07.001

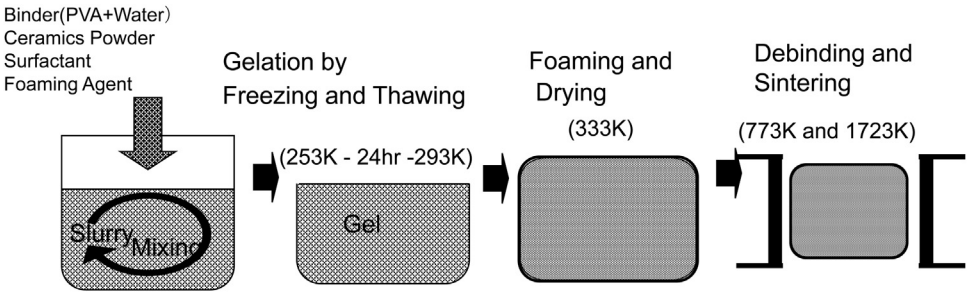

Fig. 1. GS method for producing high porosity ceramic foam.

Table 1
Ingredients for producing alumina refractory bricks.

Ingredient	Specifications
Alumina powder	a-alumina, MM-22, Nippon lightweight Metal Co. Average particle diameter of powder = 0.3 μm, Al_2O_3 99.6%
Ceramic fiber	CFP-50, ITM Co. Ceramics: Al_2O_3 48%, SiO_2 52%, fiber length < 80 mm, average diameter = 2–4 μm
Polyvinyl alcohol (PVA)	N-300, Nippon GouseiKagaku Co., m.w. = 80,000
PVA binder	10 wt% water solution of N-300 PVA
Surfactant	Yashinomi Sennzai, Saraya Co. Ltd.
Foaming agent	Normal Pentane (n-Pentane)

2. Preparation and evaluation methods of alumina foams

2.1. GS (gelation of slurry) method

Fig. 1 shows a schematic of the GS (gelation of slurry) method for production of high porosity ceramic foam. First, a slurry containing ceramic powder, foaming agent, and surfactant in an aqueous polymer solution was prepared. The aqueous polymer solution was poly vinyl alcohol (PVA) solution because it forms a strong gel after being frozen and kept 10–20 K below the re-melting point of water.[7,8] The foaming agent was pentane because its boiling point is 319 K, which is about 30 K below the re-melting temperature of the aqueous PVA solution. Next, this slurry was frozen for 24 h, and then thawed to form a gel. Then, the slurry gel was heated to about 333 K, which is the temperature that pentane starts to foam. To achieve fine foaming condition, the slurry gel must be kept from 10 to 20 K lower than its re-melting temperature. This step in the GS method caused the slurry to take on a closed-cell structure. The slurry is then dried by heating to a set temperature, thus yielding a precursor of the ceramic foam. Finally, this precursor is sintered to form a ceramic foam.

2.2. Production of a high porosity alumina refractory brick

Table 1 shows the components of the alumina foam processed according to Fig. 1 as follows. First, a slurry was prepared by mixing the binder with the alumina powder and ceramic fiber. The ceramics fiber is mixed as solid skeleton for preventing cracks while the sintering. Table 2 shows the various concentrations of foaming agent used to determine the effect on porosity of the alumina foam and shows the corresponding surfactant concentrations. Next, a slurry gel was prepared by freezing the slurry at 253 K for 24 h and then thawing at 293 K. Then, a foam was prepared by first heating the slurry gel and then drying it in a constant-temperature oven at 333 K for several days. Finally, a high porosity alumina refractory brick was then formed by debinding this precursor at 773 K for 2 h, then sintering in a furnace under atmospheric conditions at 1773 K for 2 h using the protocol shown in Fig. 2. These alumina refractory bricks contain 92.2% Al_2O_3 and 7.8 wt% SiO_2

2.3. Evaluation of structure and strength of alumina foams

The structure of the alumina foams was observed using an electron microscope (Keyence VE-9800, Japan) in 0.5 kV electron accelerating voltage. The compressive strength σ of the foams was evaluated based on compression tests using an autograph (Shimadsu AGS-10kND, Japan). In the compression test,

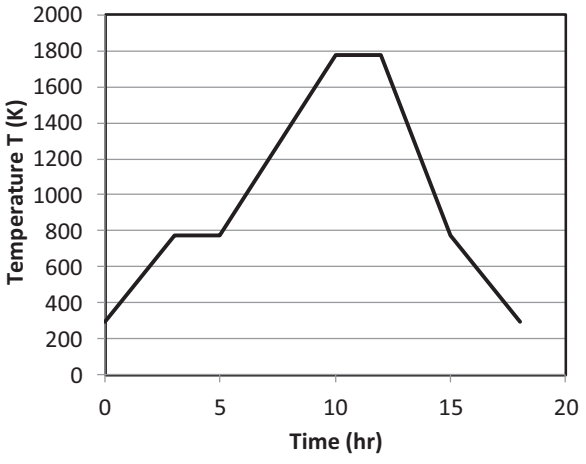

Fig. 2. Sintering protocol for producing high porosity alumina foams using GS method (Fig. 1).

Table 2
Concentrations of slurries for high porosity alumina refractory bricks.

Foam sample	Alumina powder (g)	Ceramic fiber (g)	PVA binder (ml)	Surfactant (ml)	Foaming agent (ml)
AF-1	240	40	260	12	12
AF-2	240	40	260	9	9
AF-3	240	40	260	7	7
AF-4	240	40	260	5	5

each specimen was 40 mm high and 25 mm × 25 mm in cross-section, the crosshead speed was 10 mm/min, and a laser distance meter (Keyence LK-080, Japan) was used to measure the compression distance.

2.4. Evaluation of thermal conductivity of alumina foams

The thermal conductivity λ_f of each alumina foams at room temperature was measured by the hot wire method using a QTM-500 (Kyoto Electronics Manufacturing Co. Ltd, Japan) and DP-31 sensor. In this method (shown schematically in Fig. 3), a constant electric current was applied to a heating wire, and the increase in temperature was measured by a thermocouple attached to the wire. The thermal conductivity was then estimated from the relation between the heating powder that was estimated from electric current and the temperature increase using Eq. (1).[9]

$$\lambda_f = \frac{Q}{4\pi} \ln\left(\frac{t_2/t_1}{\Delta\theta}\right) \quad (1)$$

where Q is supplied power per length (in the unit of W/m) by the hot wire, t_1, t_2 is measuring time (s) of temperature and $\Delta\theta$ is the temperature deference (K) between time t_1 and t_2.

3. Theoretical estimation of thermal conductivity of solid foam

3.1. Thermal conductivity of solid foam at room temperature

Thermal conductivity of solid foam, λ_f, is expressed as Eq. (2).[10]

$$\lambda_f = \lambda_s + \lambda_g + \lambda_c + \lambda_r \quad (2)$$

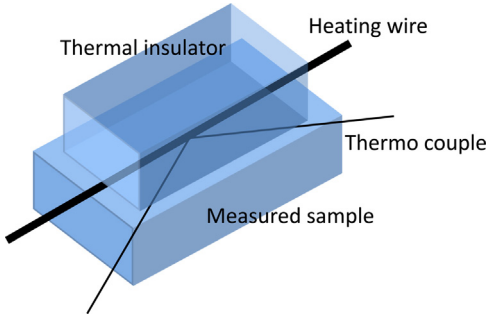

Fig. 3. Schematic of thermal conductivity measurement by hot-wire method.

where λ_s, λ_g, λ_c and λ_r are thermal conductivity through a solid, thermal conductivity through a gas in the cell, convection within the cells, and radiation through the cell walls, respectively. However, at room temperature, the effects of λ_c, λ_r are small enough to be assumed negligible. Also, thermal conductivity of air λ_{air} at room temperature is small, and estimated about 0.022 W/mK from Table 3.[11] λ_g of air is expressed Eq. (3). In high porosity, $p^{1/3} \doteqdot 1.0$.

$$\lambda_g = \lambda_{air}\, p^{1/3} \doteqdot \lambda_{air} = 0.022(\mathrm{W/mK}) \quad (3)$$

In ceramics foam, λ_s depends almost entirely on thermal conductivity by the cell structure, and thus depends on the relative density ρ_r of the foam. This relation is expressed by the Lemlich formula[12] or Ashby–Glicksman model[13,14] as

$$\frac{\lambda_s}{\lambda_d} = \xi\rho_r = \xi(1-p) \quad (4)$$

where p is porosity, λ_s is thermal conductivity through a solid part of foam, λ_d is thermal conductivity of the bulk material, ξ is parameter concern to cell structure of the foam and expressed Eq. (5).

$$\xi = \frac{2 - f_s}{3} \quad (5)$$

where f_s is the volume ratio of a strut to the total solid volume of a cell. If a cell has open cell structure consisting of only strut, then $\xi = 1/3$, whereas if a cell has closed cell structure in which the cell wall thickness and strut diameter are equal, then $\xi = 2/3$, Total thermal conductivity of foam material λ_f at room temperature is expressed Eq. (6).

$$\lambda_f = \lambda_s + \lambda_g \doteqdot \xi(1-p)\lambda_b + \lambda_{air} \quad (6)$$

3.2. Thermal conductivity of solid foam above room temperature

When the temperature of the foam is increased, thermal conductivity by heat radiation needs to be considered. The Kunii model expresses the thermal conductivity of porous material by including heat radiation as follows,[15,16] thus can be used to estimate the thermal conductivity at increased temperature as

$$\lambda_f = \lambda_s + \lambda_g + \lambda_r = (1 - p^{2/3})\lambda_d\, C + \lambda_{air}\, p^{1/3} + \left(\frac{2}{3}\right) 10^{-6}(\alpha_r\, D_p) p^{1/3} \quad (7)$$

where λ_d is thermal conductivity through the solid parts of the dense material, λ_{air} is thermal conductivity of air inside the cell,

Table 3
Thermal conductivity of air λ_{air} at elevated temperature.[11]

Temperature (K)	273	473	673	873	1073	1273
Thermal conductivity X_{air}(W/mK)	0.0205	0.0335	0.0447	0.0534	0.0602	0.0655

Table 4
Structures of high porosity alumina refractory bricks and Shrinkage ratio during sintering.

Foam sample	Porosity (%) P	Bulk density, (g/cm^3) ρ	Average cell diameter (μm) D_p	Shrinkage ratio during sintering L_s
AF-1	97.0	0.116	377	0.092
AF-2	95.9	0.159	410	0.086
AF-3	94.6	0.208	350	0.082
AF-4	93.1	0.268	305	0.097

C is a correction factor, D_p (μm) is cell diameter, and α_r is radiant heat transfer coefficient expressed as

$$\alpha_r = 0.1942\, e \left(\frac{T}{100}\right)^3 (\mathrm{W/m^2K}) \quad (8)$$

where e is thermal emissivity and T is temperature (K).

The Kunii model uses the Serial–Parallel model[17,18] expressed as follows for the thermal conductivity through a solid and a air.

$$\lambda_f = (1 - p^{2/3})\lambda_d + \lambda_{air}\, p^{1/3} \quad (9)$$

However, because Eq. (9) does not suitable for a foam whose $p > 80\%$, we modified Eq. (7) using the Ashby–Glicksman model, thus yielding the following expression for λ_f at elevated temperature:

$$\lambda_f = \xi(1 - p)\lambda_d + \lambda_{air}\, p^{1/3} + \left(\frac{2}{3}\right) 10^{-6}(\alpha_r\, D_p)p^{1/3}. \quad (10)$$

4. Results and discussion

4.1. Structure and strength of alumina foams

The porosity p of the foams was controlled by changing the foaming agent composition. Table 4 shows the measured p, ρ(g/cm^3), D_p (μm) and shrinkage ratio Ls. Fig. 4 shows photographs of the cell structure of foams of different ρ. Although the average cell diameter D_p depended on ρ, this dependency is

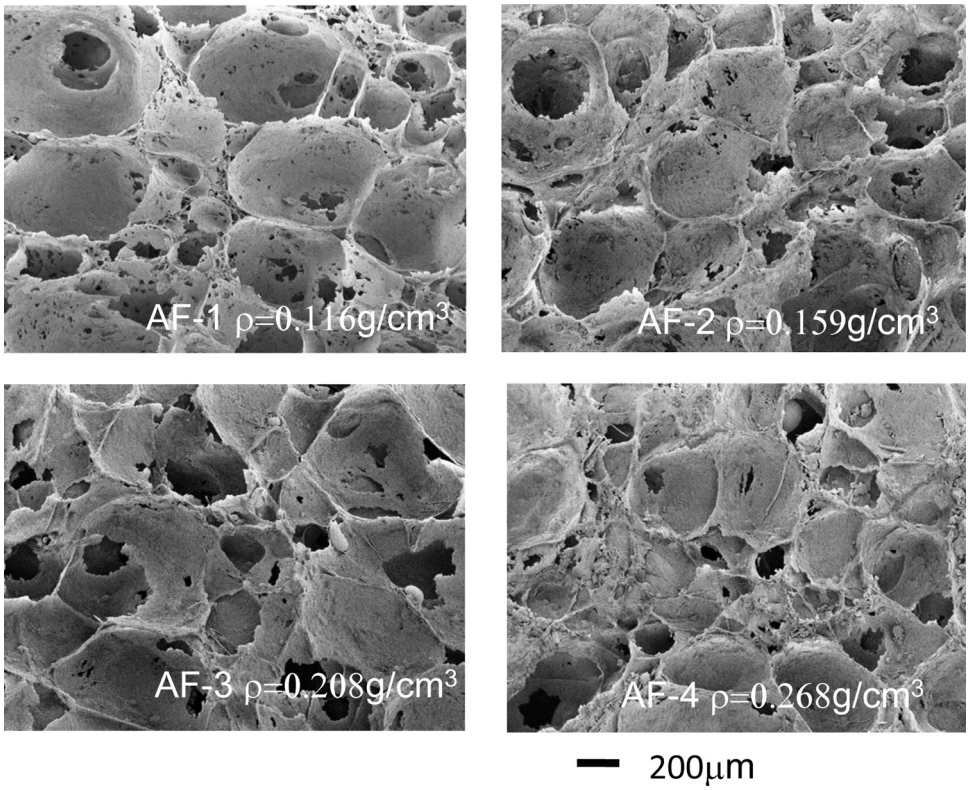

Fig. 4. Photographs of cell structure for alumina foams of different bulk density ρ.

Table 5
Thermal conductivity (W/mK) of alumina (Al_2O_3 93 wt%) at elevated temperature. Conductivity of 15.2% porosity alumina λ_f is the measured value,[21] and conductivity of 0% porosity alumina λ_b is estimated from the measured value using the Russell model.[19]

Temperature (K)	300	500	700	900	1100	1300	1500
Thermal conductivity λ_f (W/mK), $P = 15.2\%$	10.11	7.0	5.23	3.84	3.20	3.08	3.26
Thermal conductivity λ_b(W/mK), $P = 0\%$	12.32	8.54	6.38	4.68	3.90	3.76	3.98

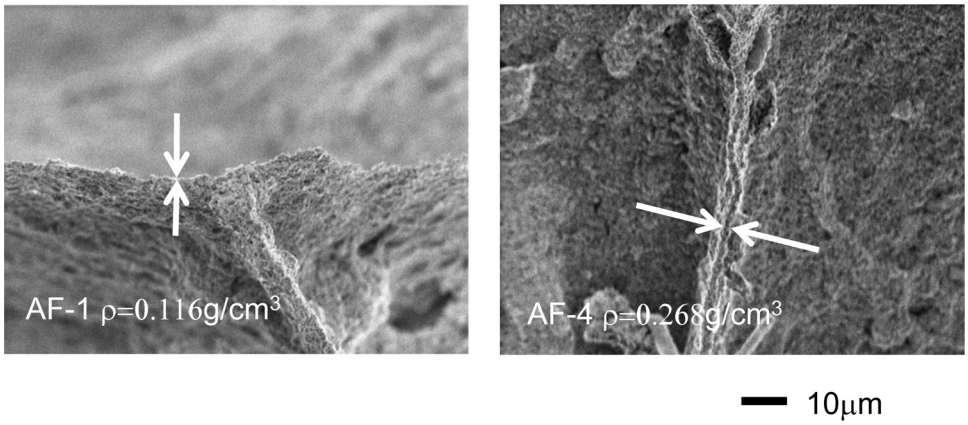

Fig. 5. Photographs of representative cell walls and thickness of alumina foam of different bulk density ρ.

not clear in these photographs. The foams exhibit a closed cell structure, although cell walls were torn in spots thus making these foams permeable to air. Based on images of representative cell walls (Fig. 5), the estimated thickness of cell walls is about 0.3–1.0 μm. In the fabrication process, the alumina particles were arranged very thin on the cell walls. Fig. 6 shows the compression test results as stress–strain (σ–ε) curves. Fig. 7 shows the effect of ρ on σ(MPa), where both axes are logarithmic scales and σ was evaluated at $\varepsilon = 0.05$ and 0.1. Based on Fig. 7, $\sigma \propto \rho^2$.

4.2. Thermal conductivity of alumina foams

Fig. 8 shows the effect of ρ on the measured thermal conductivity λ_f of alumina foam prepared by the GS method at room temperature, and also shows the thermal conductivity λ_s estimated from Eq. (2). The thermal conductivity λ_d of dense alumina foam (93 wt% Al_2O_3) at room temperature (12.32 W/mK) is estimated using the Russell model[19] by Eq. (11) and thermal conductivity λ_s of 15.2% porosity 93 wt% Al_2O_3 at room temperature (10.11 W/mK) that was previously measured:[20]

$$\frac{\lambda_s}{\lambda_d} = \frac{1 - p^{2/3}}{1 + p - p^{2/3}} \tag{11}$$

The figure shows that when $\xi = 1/3$, the estimation by Eq. (3) (solid lines) is similar to the measured results (solid squares), because the cell wall is very thin and has small volume, and that result, f_s is almost 1.0.

Fig. 9 shows λ_f of the different alumina foams measured at different temperatures from room temperature to 1173 K. The thermal conductivity λ_d of alumina decreased with increasing temperature, whereas λ_r increased proportionally to the temperature to the third power. The alumina foams thus exhibited parabolic λ_f curves, which are also observed in λ_f of alumina fibers.[21] The λ_f of the foams above room temperature was estimated using the modified Kunii model in Eq. (10). Table 5 shows λ_d of dense alumina (Al_2O_3 93 wt%) above room temperature estimated from measured λ_f of 15.2% porosity alumina bricks[20] and Eq. (11). Alumina has high λ_d, which decreases with increasing temperature.[22] Table 3 shows λ_{air}.[11] In the GS method, p could be controlled by concentration of foaming agent in the slurry, and thus the relation between the average D_p and p can be expressed as

$$D_p{}^3(1 - p) = \text{const.} \tag{12}$$

Fig. 10 shows the estimated λ_f of the alumina foams above room temperature, assuming $D_p{}^3(1 - p) = 2.0 \times 10^6(\mu m^3)$. Again, a parabolic curve is exhibited. However, λ_g by radiation was underestimated, because the cell walls of the foams were thin and sometimes torn, which would enhance the effect

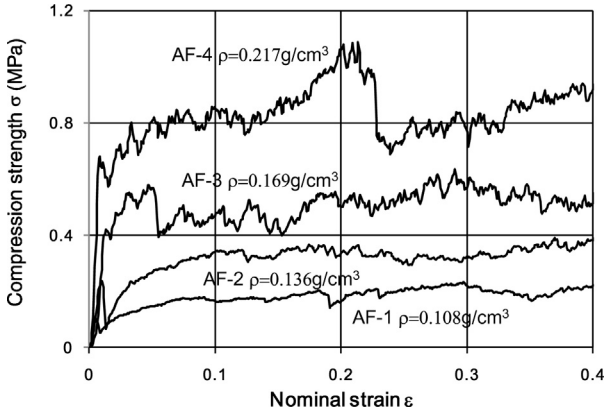

Fig. 6. Stress–strain (σ–ε) curves of alumina foams during compression tests.

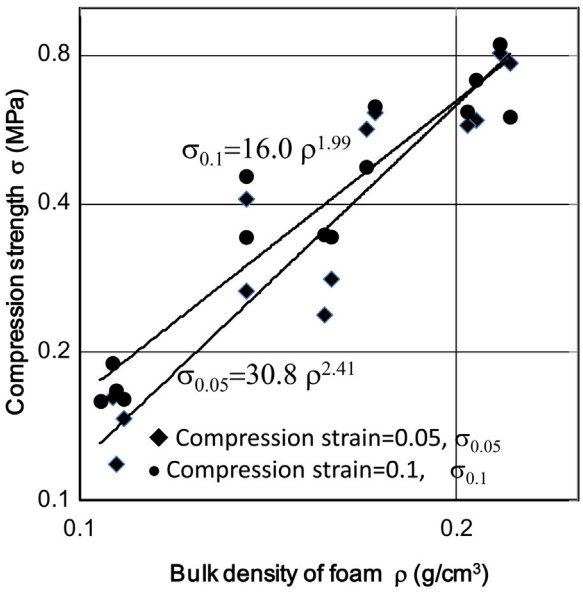

Fig. 7. Bulk density ρ vs. compression strength σ of alumina foams produced by GF method.

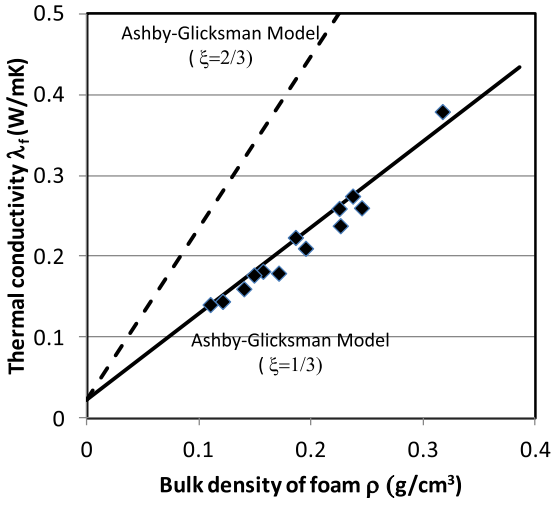

Fig. 8. Bulk density ρ vs. thermal conductivity λ_f of alumina foam at room temperature.

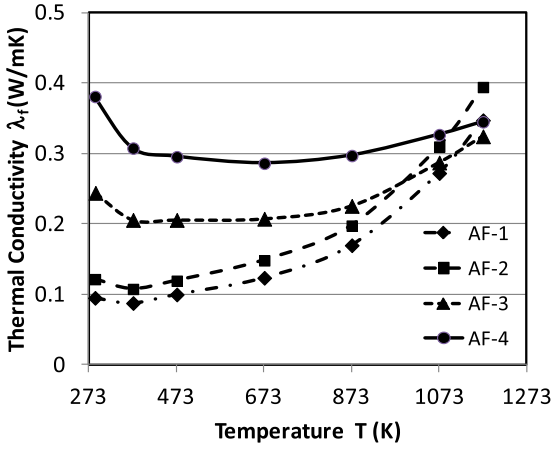

Fig. 9. Thermal conductivity λ_f of alumina foams above room temperature.

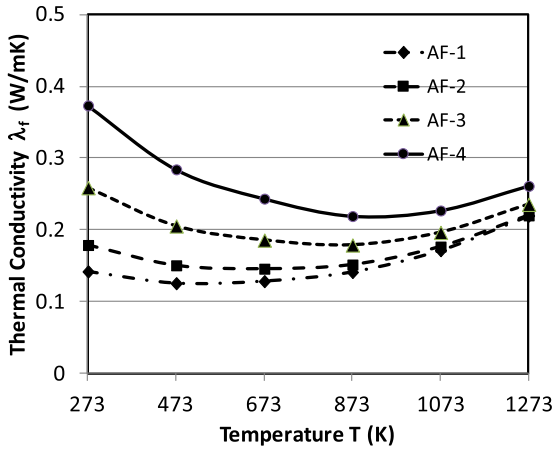

Fig. 10. Thermal conductivity λ_f of alumina foams estimated using the modified Kunii model (Eq. (7)) above room temperature.

of radiation on conductivity. For more exact estimation of thermal conductivity, precise discussion about radiative heat transfer of foam materials[23] will be necessary.

5. Conclusions

High porosity alumina refractory bricks can be produced using the GS method in which foam with 90–97.5% porosity could be fabricated. These foams have high compression strength from 0.2 to 3 MPa, which is proportional to the square of the bulk density. At room temperature, they also have low thermal conductivity (from 0.1 to 0.4 W/mK) that is proportional to the bulk density and can be expressed using the Ashby–Glicksman model. In the foams at temperatures above room temperature, the thermal conductivity by the solid portions of alumina is reduced, whereas conduction by radiation is increased. Consequently, an optimum foam density must be determined so as to maintain low thermal conductivity from room temperature to high temperature. The thermal conductivity of these foams can be estimated relatively well by the modified Kunii model.

References

1 Katsube K, Hashida M, Tenra T. Development of high-performance vacuum insulation panel. Matsushita Tech J 2006;52(6):482–5.
2 Marukoshi Co. Product Catalogs.
3 Zivcova Z, Gregorova E, Pabst W, Smith DS, Michot A, Poulier C. Thermal conductivity of porous alumina ceramics prepared using starch as a pore-forming agent. J Eur Ceram Soc 2009;29:347–53.
4 Shimizu T, Matsuzaki K. Metal foam production process using hydro-gel and its improvement. Mater Sci Forum 2007;539–543:1845–50.
5 Shimizu T, Matsuzaki K, Kikuch K, Kanetake N. Method to produce high porosity metal foam using gelation of water base binder. J Jpn Soc Powder Powder Metallurgy 2010;57:227–83.
6 Shimizu T, Matsuzaki K, Kikuchi K, Kanetake N. Method to produce high porosity metal foam using gelation and effect of used powder grain size. J Jpn Soc Powder Powder Metallurgy 2010;57:284–90.
7 Watase M, Nishinari K. Large deformation of hydrogels of poly(vinyl alcohol), agarose and *kappa*-carrageenan. Macromol Chem Phys 1985;186:1081–6.

8 Lozinsky VI, Plieva FM. Poly(vinyl alcohol) cryogels employed as matrices for cell immobilization. 3. Overview of recent research and developments. Enzyme Microb Technol 1998;23:227–42.
9 Coquard R, Baillis D, Quenard D. Experimental and theoretical study of the hot-wire method applied to low-density thermal insulations. Int J Heat Mass Transfer 2006;49:4511–24.
10 Gibson LJ, Ashby MF. Cellular solid structure and properties. 2nd ed Cambridge: Cambridge University Press; 1997.
11 Kunii D. Thermal conductivity of powder. J Jpn Soc Chem Eng 1961;25:892–8.
12 Lemlich R. A theory of the limiting conductivity of polyhedral foam at low density. J Colloid Interface Sci 1978;64:107–10.
13 Ewaire D, Hutzler S. The physics of foam. New York: Oxford University Press; 1999.
14 Glicksman LR. Heat transfer in foams. In: Hilyard NC, Cunningham A, editors. Low density cellular plastics. London: Chapman & Hill; 1994. p. 104–52.
15 Kunii D. Thermal conductivity of porous media by radiation. J Jpn Soc Mech Eng 1962;65–525:1447–53.
16 Kunii D, Smith JM. Heat transfer characteristics of porous rocks. J Am Inst Chem Eng 1960;6:71–7.
17 Leach AG. The thermal conductivity of foams. I. Models for heat conduction. J Phys D Appl Phys 1993;26:733–9.
18 Abramenko AN, Kalinichenko AS, Burtser Y, Kalinichenko VA, Tanaeva SA, Vasilenko IP. Determination of the thermal conductivity of foam aluminum. J Eng Phys Thermophys 1999;72(3):369–73.
19 Russell HW. Principles of heat flow in porous insulators. J Am Ceram Soc 1935;18(1):1–5.
20 Okazaki M, Imakoma H. Porous materials characterization, production and application. Tokyo: Fuji Techno System; 1999.
21 Hayashi K, Fujino Y, Nishikawa T. Thermal conductivity of Aluminium and Zirconia fiber insulators at high temperature. Yogyo Kyokai Shi 1983;91:450–6.
22 Japan Themophysics Society ed. Thermophysical property handbook. Tokyo: Yokendo; 1990.
23 Kaemmerlen A, Vo C, Asllanaj F, Jeandel G, Baillis D. Radiative properties of extruded polystyrene foam: Predictive model and experimental results. J Quant Spectrosc Radiat Transfer 2010;111:865–77.

Toru Shimizu He received B.S. degree in 1979 from Nagoya Universsity, Nagoya, Japan, and starts a research work as a researcher at Mechanical Engineering Laboratory, Agency of Industrial Science and Technology (AIST), Ministry of International Trade and Industry, Japanese Government. He was a Senior Researcher from 1988. Form 1990 to1991, He was a visiting researcher of CEMEF, Ecole National Sperieure des mines de Paris, Sphia Antipolis, France. In April 2001, Agency of Industrial Science and Agency was revitalized, and becomes National Institute of Advanced Industrial Science and Technology (AIST), and he was a senior researcher of AIST.

His areas of research interest are Metal forming and forging, Computer simulation of forging process, Powder metallurgy, Powder injection molding process, their debinding process using CO_2 Supercritical fluid, Additive manufacturing process using powder materials and Metal or ceramics foam production process from powder materials.

Membership of academic societies: JSTP (The Japanese Society for Technology of Plasticity) Member, Editor of the Journal, Past member of administrative board; JIM (The Japan Institute of Metals) Member; JSPM (Japan Society of Powder and Powder Metallurgy) Member, Member of administrative board; JSCES (The Japan Society for Computational Engineering and Science) Member.